Effect of Heme Binding on the Structure and Stability of *Escherichia coli* Apocytochrome b_{562}[†]

Yiqing Feng and Stephen G. Sligar*

Departments of Biochemistry, Chemistry, and Biophysics, University of Illinois, Urbana, Illinois 61801

Received May 21, 1991; Revised Manuscript Received July 31, 1991

ABSTRACT: The structure and stability of apocytochrome b_{562} were explored using absorption and circular dichroism spectroscopic methods. The polypeptide chain retains a well-defined structure when the prosthetic heme group is removed from cytochrome b_{562}. Circular dichroism measurements estimate 60% helicity for apocytochrome b_{562}, compared with 80% helicity found in holocytochrome b_{562}. At low pH, apocytochrome b_{562} displays a midpoint pH of 2.9, while ferricytochrome b_{562} displays a midpoint pH of 2.3. The unfolding of the apoprotein by urea and heat can be well approximated by the two-state transition model. The stability of apocytochrome b_{562} is significantly reduced from that of the holoprotein. The free energy of stabilization ($\Delta G°$) and the midpoint transition temperature (T_m) for apocytochrome b_{562} are found to be 3.2 ± 0.5 kcal/mol and 52.3 ± 0.9 °C, respectively, compared with 6.6 ± 0.5 kcal/mol and 67.2 ± 0.5 °C for ferricytochrome b_{562}. The smaller heat capacity change upon unfolding of apocytochrome b_{562} than that of ferricytochrome b_{562}, estimated from the thermodynamic parameters, indicates that apocytochrome b_{562} possesses a smaller hydrophobic core than holocytochrome b_{562}. Size-exclusion chromatography studies indicate that the apoprotein is slightly more extended in molecular dimension than ferricytochrome b_{562}. The data suggest that apocytochrome b_{562} resembles a "molten globule" or a "collapsed form" of the holoprotein, in which secondary structure formation is largely complete while the global folding is either only partially complete or dynamically expanded.

Cytochrome b_{562} is a small soluble protein (12.3 kilodaltons) isolated from *Escherichia coli* and contains a *b*-type heme prosthetic group (Itagaki & Hager, 1966). Its biological function is thought to be electron transfer, although in *E. coli* the identity of the physiological partners remains unknown. X-ray crystallographic studies revealed that ferricytochrome b_{562} exists as a four-helix bundle, with the helices packed nearly antiparallel to each other (Mathews et al., 1979; Lederer et al., 1981). The heme is bound to the N- and the C-terminal helices through a histidine/methionine ligation and is located at one end of the bundle.

The simplicity of cytochrome b_{562} structure renders it a good model to study protein stability and folding. In addition to the folding information encoded in the primary sequences, the complete folding of the cytochromes and globins also requires the binding of the heme prosthetic group. Earlier studies on apomyoglobin [e.g., see Griko et al. (1988)], apohemoglobin [e.g., see Yip et al. (1972) and Leutzinger and Beychok (1981)], and apocytochrome b_5 [e.g., see Huntley and Strittmatter (1972)] have demonstrated that the structure and stability of these proteins depend strongly on the presence of the heme. Although the apoprotein structures are distinct from the native holoprotein, they are clearly distinguishable from completely unfolded polypeptide chains. More recent NMR studies on apocytochrome b_5 and apomyoglobin (Moore & Lecomte, 1990; Cocco & Lecomte, 1990; Moore et al., 1991) suggest that the hydrophobic cores present in these native holoproteins are at least partially retained. These apoprotein structures might be physiologically significant folding intermediate states of the corresponding holoproteins, if a post-translational heme insertion takes place in vivo. Despite previous efforts, our current understanding of the effect of prosthetic groups on protein folding is rather limited. The presence of the heme prosthetic group in cytochrome b_{562} provides us with the opportunity to explore the role of heme on the integrity and folding of the native structure. The large amount of regular secondary structure present in cytochrome b_{562} is expected to simplify the understanding of these issues.

Concurrent with our high-resolution NMR studies of apocytochrome b_{562} structure, we have carried out a structural and thermodynamic characterization of the apoprotein using optical spectroscopic techniques. The success of cloning the cytochrome b_{562} gene and the development of a high-level bacterial expression system have made available large quantities of pure protein for biophysical characterizations (Nikkila et al., 1991). In this paper, we report the structural and thermodynamic properties of apocytochrome b_{562} obtained using ultraviolet/visible absorption, circular dichroism, and gel filtration methods. The results show that the stability of the protein is considerably reduced following the removal of the heme, and although a large portion of the helicity is retained in apocytochrome b_{562}, the structure is more extended and possesses a smaller hydrophobic core than the holoprotein does.

Materials and Methods

Sample Preparation. Cytochrome b_{562} was obtained from *Escherichia coli* strain TB-1 harboring pNS207 grown in LB and was purified as previously described (Nikkila et al., 1991) with some modifications. The harvested cells were resuspended in 10 mM Tris/1 mM EDTA, pH 8.0, buffer and were subject to a chloroform extraction (Ames et al., 1984). Upon centrifugation, the supernatant containing cytochrome b_{562} was titrated to pH 4.55 and was stirred for a minimum of 1 h at 4 °C. The precipitate was removed by centrifugation, and the supernatant was brought to neutral pH. After being concentrated to a small volume, the supernatant was loaded onto

[†]This work was supported by National Institutes of Health Grant GM31756 and the University of Illinois Materials Research Laboratory supported by NSF DMR 8920538.

* To whom correspondence should be addressed.

0006-2960/91/0430-10150$02.50/0

a Bio-Gel P30 (Bio-Rad) gel filtration column equilibrated with buffer containing 20 mM potassium phosphate/0.2 mM EDTA, pH 7.4. The eluted fractions were then applied to a DEAE-cellulose (Sigma) ion-exchange column equilibrated with the same buffer and eluted with a salt gradient of 0–200 mM KCl. The protein used in this study had a ratio of 6.1 for A_{418}/A_{280} in the oxidized state and a ratio of 1.60 for A_{562}(reduced)/A_{280}(oxidized).

The apoprotein was prepared at 4 °C using the butanone extraction method (Teale, 1959). Typically, 10–40 mg of cytochrome b_{562} in 10 mL of 20 mM phosphate/0.2 mM EDTA, pH 7.4, was titrated to pH 2.0 by adding 2.0 N ice-cold HCl. Equal volumes of butanone, prechilled to −20 °C, were used repeatedly to extract the red heme until the butanone layer became colorless. The apoprotein was dialyzed against 100 mM phosphate/0.1 mM EDTA, pH 7.0, for 24 h with several buffer changes. The protein was concentrated and was either used immediately or stored at liquid nitrogen temperature. The apoprotein obtained contains less than 2% holoprotein, as judged from the Soret absorbance peak.

For ferrocytochrome b_{562} samples, a minimum amount of sodium dithionite was added to the sample prior to the measurements. The oxidation state of the protein was monitored after the experiments and was found to be >98% reduced.

Cytochrome b_{562} concentrations were determined by measuring the Soret absorbance at 418 nm in the ferric state or at 427 nm in the ferrous state, using extinction coefficients of 117.4 and 180.1 mM^{-1} cm^{-1}, respectively (Itagaki & Hager, 1966). The apocytochrome b_{562} concentration was determined by measuring the UV absorbance at 277 nm, using an extinction coefficient of 3.0 mM^{-1} cm^{-1} derived from the aromatic residue composition of the protein under both neutral and alkaline conditions (Edelhoch, 1967).

Absorption Spectroscopy. Absorption spectra were measured on a Hewlet-Packard 8450 rapid-scan diode array spectrophotometer equipped with a Hewlett-Packard 89101A thermostated cell holder and a 89100A temperature-control station. For the thermal unfolding experiments, spectral changes were recorded during a programmed temperature ramp at 2° C increments. The solution was equilibrated at each temperature for 2 min prior to recording a spectrum for 60 s. The temperature of the sample during the experiments was measured using a YSI thermometer and probe.

Circular Dichroism Spectroscopy. The CD measurements were performed in fused quartz cuvettes with 0.1-cm path length, purchased from Hellma, on a SPEX CD6 spectropolarimeter interfaced with an IBM AT computer. For the urea denaturation curves, the mean residue ellipticity at 222 nm was recorded for 10 s at each urea concentration. The thermal unfolding curves were measured with a water-jacketed cuvette by increasing the temperature at 2.5 °C per step, followed by 2.5-min equilibration, and then recording for 1 min. The temperatures reported were directly monitored in the solution during the experiments. Protein concentrations for CD measurements ranged from 6 to 15 μM. Base lines obtained from samples containing buffer only were subtracted from all the data presented. To estimate secondary structure composition, circular dichroism spectra were recorded from 190 to 250 nm with an increment of 0.2 nm (for the apoprotein and the ferric protein) or 0.5 nm (for the ferrous protein) and a response time of 1 s. A spectrum was typically averaged for five scans. The spectra were analyzed without applying any data smoothing routine using the CONTIN application package (Provencher & Glockner, 1982) kindly provided by Dr. Provencher.

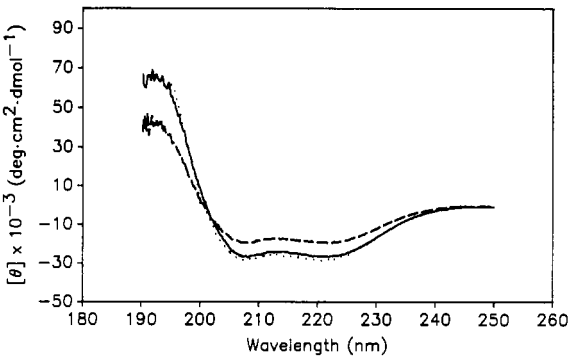

FIGURE 1: Far-UV circular dichroism spectra of ferricytochrome b_{562} (—) and apocytochrome b_{562} (- - -) in 100 mM potassium phosphate and of ferrocytochrome b_{562} in 10 mM potassium phosphate (···), pH 7.0 at 22 ± 0.5 °C. The protein concentrations were 8–10 μM. No data smoothing routine was applied.

Acid and Urea Unfolding. For acid unfolding studies, the stock protein was added to buffer solutions with the pH preadjusted using minimal amounts of HCl. The pH values reported were measured after the experiments. Stock solution of urea was freshly prepared prior to the experiments. For urea denaturation studies of the apoprotein, samples were incubated at room temperature (ca. 22 °C) for a minimum of 1 h prior to the measurements. An incubation time of 5–8 h was used for denaturation of the oxidized protein. The urea denaturation curves were analyzed by assuming a two-state transition model using a nonlinear least-squares fitting routine. First-order base-line corrections were applied when appropriate. Ultrapure urea was purchased from United States Biochemical Corp.

Size-Exclusion Chromatography. An HPLC system equipped with a TSK G3000SW gel filtration column (7.5 mm × 30 cm) was used in this study. Buffer solution of 100 mM potassium phosphate, pH 7.0, was used throughout the experiments. The injection volume was 200 μL, and the flow rate was 0.7 mL/min.

Surface Area Calculation. The solvent-accessible surface area of cytochrome b_{562} was calculated using the programs ACCESS and ACCFMT kindly provided by Dr. F. M. Richards. The calculations were performed on the newly refined high-resolution crystal structure of ferricytochrome b_{562} kindly provided by Dr. F. S. Mathews.

RESULTS

Circular Dichroism Spectra and Secondary Structure Composition. Far-UV circular dichroism spectra of ferri-, ferro-, and apocytochrome b_{562} are shown in Figure 1. The strong negative peak at 222 nm in all three spectra is indicative of high helical contents. The spectrum of ferrocytochrome b_{562} is practically identical to that of ferricytochrome b_{562}. The spectrum of apocytochrome b_{562}, however, shows a decrease in ellipticity, indicating less helical content compared with the holoprotein. For the protein in three states (i.e., ferri, ferro, and apo), differences resulting from the ionic strength changes are minimal. Contrary to a previous report (Myer & Bullock, 1978), the dramatic change in the CD spectra of ferrocytochrome b_{562} between 10 and 100 mM potassium phosphate buffers was not observed in our experiments.

Upon fitting the CD spectra, the helical contents were estimated to be 82% and 59% for ferricytochrome b_{562} and apocytochrome b_{562}, respectively (Table I). In addition to the reduced helicity, apocytochrome b_{562} displays a small amount of β-sheet conformation. The spectrum of ferrocytochrome b_{562} was not used for direct fitting due to poor signal to noise at low wavelengths, resulting from the strong

Table I: Secondary Structure Compositions[a]

sample	% α-helix	% β-sheet	% random coil
ferricytochrome b_{562}	82	0	18
apocytochrome b_{562}	59	12	29

[a] Estimated from CD spectra of the above proteins in 100 mM potassium phosphate, pH 7.0, as described under Materials and Methods.

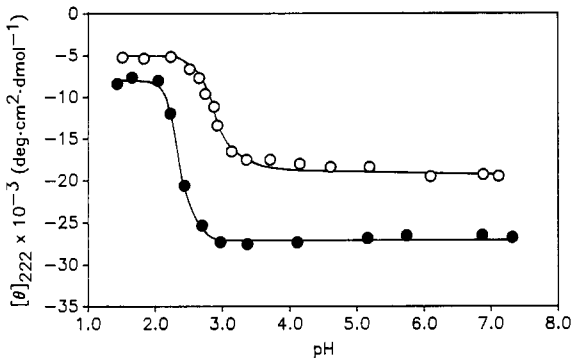

FIGURE 2: Acid denaturation of apocytochrome b_{562} (○) and ferricytochrome b_{562} (●) at 20 ± 0.2 °C. The mean residue ellipticity $[\theta]_{222}$ is plotted as a function of pH. Samples contained 8 μM protein, 2 mM sodium citrate, and 5 mM glycine. The solid lines are drawn by inspection.

absorption of dithionite. The secondary structure composition of ferrocytochrome b_{562} is assumed to be similar to that of ferricytochrome b_{562}, since their CD spectra are essentially identical.

Acid Unfolding. The unfolding of apocytochrome b_{562} at low pH was monitored at $[\theta]_{222}$ (Figure 2). The transition midpoint was found to be ca. pH 2.9. In comparison, the acid unfolding of ferricytochrome b_{562}, monitored at both the Soret absorption peak (data not shown) and the mean residue ellipticity at 222 nm (Figure 2), shows a similar pattern but with a somewhat lower transition midpoint (ca. pH 2.3). Upon immediate return to neutral pH, apocytochrome b_{562} refolds to approximately 90%, while the refolding of ferricytochrome b_{562} reaches 81% assessed by CD but 36% assessed by Soret absorbance intensity. The Soret intensity reaches 50% in 17 h at 4 °C.

Free Energy of Stabilization. To characterize the stability of apocytochrome b_{562}, a denaturation curve was generated by measuring $[\theta]_{222}$ as a function of urea concentration (Figure 3A). Using the two-state transition model, the data were fitted to the equation:

$$\Delta G = -RT \ln K = -RT \ln [(y_N - y)/(y - y_U)] \quad (1)$$

where ΔG is the free energy of unfolding, K is the equilibrium constant, y is the observed signal, and y_N and y_U are the signals in the native and unfolded states, respectively. A further assumption was made that

$$\Delta G = \Delta G^0 - m[\text{denaturant}] \quad (2)$$

where ΔG^0 is the free energy of stabilization in the absence of denaturant (Schellman, 1987) and m is a measure of the dependence of ΔG on denaturant concentration. At 20 °C, the free energy of stabilization obtained for apocytochrome b_{562}, extrapolated to zero urea concentration, is 3.2 ± 0.5 kcal/mol. (The errors indicated here and below are derived from calculations using different data sets.)

The denaturation curve of ferricytochrome b_{562} as monitored at the Soret absorbance peak at increasing urea concentrations is shown in Figure 3B. The data were analyzed as described above, and the best fit was obtained with a free energy of stabilization of 6.6 ± 0.5 kcal/mol. The urea-induced unfoldings of both apocytochrome b_{562} and ferricytochrome b_{562} are completely reversible.

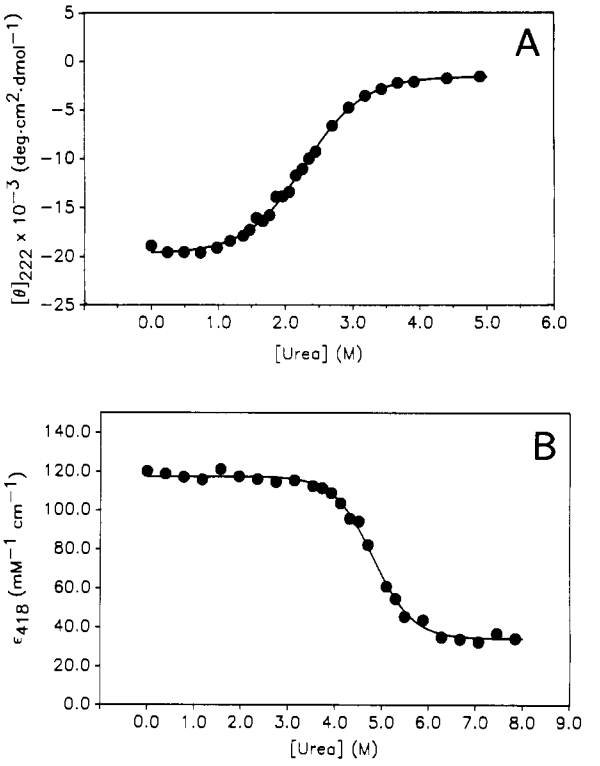

FIGURE 3: Urea-induced denaturation curves of apocytochrome b_{562} (A) and ferricytochrome b_{562} (B) at 20 ± 0.2 °C. (A) The mean residue ellipticity $[\theta]_{222}$ is plotted as a function of urea concentration. Samples contained 10 μM apocytochrome b_{562} and 50 mM potassium phosphate, pH 7.0, in addition to urea. (B) The extinction coefficient at 418 nm is plotted as a function of urea concentration. The samples contained 8 μM ferricytochrome b_{562} and 50 mM phosphate, pH 7.0, in addition to urea. Solid lines represent the nonlinear least-squares fit to a two-state transition model (zero-order base lines were used).

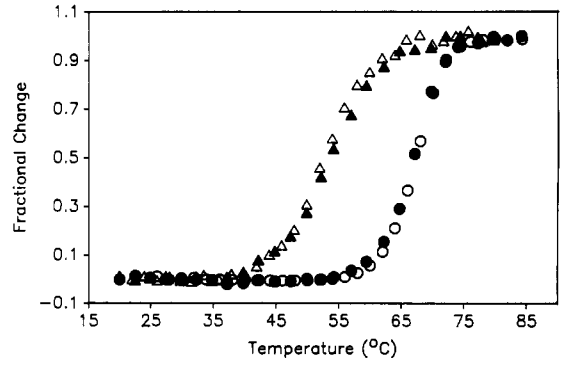

FIGURE 4: Normalized thermal denaturation curves of apocytochrome b_{562} and ferricytochrome b_{562}. The fractions of denatured protein were plotted as a function of temperature for apocytochrome b_{562} measured by the near-UV difference spectroscopic method at 286 nm (△) and by circular dichroism at 222 nm (▲) and for ferricytochrome b_{562} measured at the Soret absorbance peak 418 nm (○) and at circular dichroism signal $[\theta]_{222}$ (●). Samples contained 50 mM phosphate, pH 7.0, and 50–60 μM protein for the UV method and 8–15 μM protein for the other measurements.

Thermal Stability. The unfolding of apocytochrome b_{562} upon heating was monitored by measuring the mean residue ellipticity at 222 nm as well as the second-derivative near-UV absorbance spectrum (Figure 4). Cytochrome b_{562} contains two phenylalanines and two tyrosines. The second-derivative UV spectral change at elevated temperature indicates the increased solvation occurring at the aromatic side chains (Demchenko, 1986). Both probes presented identical transition

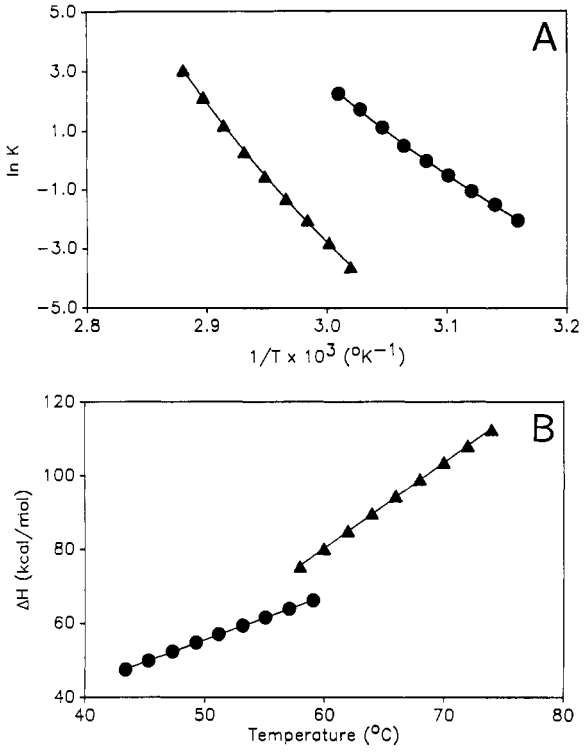

FIGURE 5: (A) van't Hoff plots of the thermal denaturation data of apocytochrome b_{562} monitored by second-derivative UV difference spectroscopy (●) and of ferricytochrome b_{562} monitored by the Soret absorbance peak (▲). The experimental condition is as in Figure 4. The solid lines are the least-squares fit of the data points using a third-order polynomial equation. (B) Dependence of enthalpy on temperature. Symbols are as in (A). ΔH values were obtained from the first derivative of the curves in (A). The slope of the least-squares fit indicates the change in heat capacity upon unfolding.

profiles. Assuming that the transition involves only the native and the denatured states, the data were analyzed using the equations:

$$d(-R \ln K)/d(1/T) = \Delta H \quad (3)$$

$$d(\Delta H)/d(T) = \Delta C_p \quad (4)$$

The analysis yields a T_m of 52.3 ± 0.9 °C, a ΔH_m of 53 ± 4 kcal/mol, and a ΔC_p of 1.1 ± 0.3 kcal/(mol·deg) (Figure 5).

These results were independent of the temperature ramping rate. Thermal unfolding curves generated at three different ramping rates (0.3, 0.5, and 1.0 °C/min) using the second-derivative UV method were found to be essentially identical. The percentage of recovery upon returning to ambient temperature, however, decreased at slower ramping rates, presumably due to damage to the protein or aggregation at prolonged exposure to high temperature. At the rate of 1.0 °C/min, the recovery of apocytochrome b_{562} exceeded 90%. Similar behavior was observed for holocytochrome b_{562} (Fisher, 1991). The two-step thermal transition profile of ferricytochrome b_{562} reported by Myer and Bullock (1978) was not observed in our experiments.

The thermal unfolding of ferricytochrome b_{562} was monitored by the mean residue ellipticity at 222 nm and the Soret absorbance peak at 418 nm. The curves generated using the two probes are identical and yield a T_m of 67.2 ± 0.5 °C, a ΔH_m of 94 ± 5 kcal/mol, and a ΔC_p of 2.4 ± 0.4 kcal/(mol·deg).

Chromatography Studies. The elution of apocytochrome b_{562} from the size-exclusion gel filtration column gives an apparent molecular weight of 18.7K upon calibration. Ferricytochrome b_{562} elutes slightly more slowly than the apoprotein, corresponding to an apparent molecular weight of 18.1K. The retention times for apocytochrome b_{562} and ferricytochrome b_{562} were independent of the protein concentration between 15 and 150 μM.

Discussion

Secondary Structure Estimations. The circular dichroism spectrum of apocytochrome b_{562} illustrates that the dominance of helical conformation in the holoprotein is retained after the removal of the heme. There are, however, approximately 20 fewer residues in the helical conformation than the holoprotein according to the CD data. A similar decrease in helicity has been observed for the myoglobin–apomyoglobin system (Harrison & Blout, 1965). It appears that the formation of a large portion of the secondary structure in cytochrome b_{562} does not require the presence of the heme. Although the location of the helices cannot be obtained from the CD studies, our high-resolution NMR investigation of apocytochrome b_{562} (Feng et al., 1991) has established that the location of the helical segments in the apoprotein coincides with those in the holoprotein crystal structure. The NMR results, however, suggest a somewhat higher percentage of helix-like conformation (ca. 70%) than ca. 60% estimated from the CD data. The small discrepancy perhaps is within the uncertainty of the CD method, although the possibility of stabilization of secondary structure by oligomer formation at the millimolar NMR protein concentrations cannot yet be completely ruled out.

The helical content estimated for the holoproteins (ca. 80%) is significantly higher than the results reported previously (ca. 50%) (Bullock & Myer, 1978), perhaps due to the different methods employed in the spectral analyses. The CD spectral analysis used here is based on present state-of-art methodology using a linear combination of the CD spectra of 16 proteins whose secondary structures have been well-defined by X-ray crystallographic studies (Provencher & Glockner, 1982). The new estimate for the holoprotein is in good agreement with the 77% helix obtained from the newly refined crystal structure (F. S. Mathews, personal communication).

Our CD studies found that the conformations of ferricytochrome b_{562}, ferrocytochrome b_{562}, and apocytochrome b_{562} are independent of ionic strength. The insensitivity of cytochrome structure to ionic strength has also been observed by the 2D NMR method in cytochrome *c* (Feng & Englander, 1990). The reason for the inconsistency of the result for ferrocytochrome b_{562} in 10 mM phosphate buffer (Myer & Bullock, 1978) remains unknown.

Unfolding Behavior at Low pH. Unfolding of proteins at low pH is believed to be the result of charge repulsion (Goto et al., 1990). For apocytochrome b_{562}, the unfolding appears to take place when the carboxyl groups are neutralized near pH 3. The lower transition midpoint (ca. pH 2.3) of ferricytochrome b_{562} may be rationalized by drawing an analogy to cytochrome *c*. Cytochrome *c* is also six-coordinated and has the same histidine/methionine ligand combination. It was proposed that the ligated His-18 imidazole in cytochrome *c* has an unusually low and ionic strength dependent p*K* (2.5 at 0.01 M Cl^{-1}; 1.4 at 0.1 M Cl^{-1}). The protonation at this site and therefore the heme dissociation are coupled to the global unfolding of cytochrome *c* (Dyson & Beattie, 1981). If ferricytochrome b_{562} behaves similarly, the ligated His-102 will have a low p*K* under our condition, leading to heme dissociation and protein unfolding near pH 2.3.

In the case of ferricytochrome b_{562}, the percentage of immediate recovery upon returning to neutral pH appears higher when measured by the mean residue ellipticity at 222 nm than

by Soret absorbance. This can be accounted for by the presence of the recovered apoprotein. Since the heme is noncovalently attached to cytochrome b_{562}, the apoprotein and the heme can separate when the axial ligands detach at low pH. On neutralization, there appears to be a lag in the heme rebinding, while the apoprotein refolds rapidly and contributes to the ellipticity.

Molecular Dimensions by Chromatography. The ferricytochrome b_{562} crystal structure can be described as a cylinder 25 Å in diameter and 50 Å in length (Mattews et al., 1979). The asymmetric shape of the molecule leads to a higher apparent molecular weight (MW_{app}) in the gel filtration experiment (MW_{app} = 18.1K, MW = 12.3K). The monomeric state of the protein is confirmed by the concentration independence of the retention time. In the gel filtration chromatography study, apocytochrome b_{562} presents ca. 600 higher apparent molecular weight than ferricytochrome b_{562}, despite the decrease in real molecular weight due to the loss of the heme (ca. 600). The following three possibilities can lead to higher apparent molecular weight: (1) dimerization of apocytochrome b_{562}; (2) a more asymmetric shape than ferricytochrome b_{562}; (3) an overall expansion of the native cytochrome b_{562} structure in the absence of the heme.

Dimerization might occur in apocytochrome b_{562} due to the exposure of the hydrophobic core when the heme is removed. Nevertheless, the difference in apparent molecular weight between the apoprotein and the holoprotein is too small for the former to be a dimer. The lack of concentration dependence of the retention time is consistent with a monomeric state. Further evidence of the monomeric state comes from NMR studies of apocytochrome b_{562} at even higher protein concentrations used in the NMR experiments. The rate of NOE buildup indicates that the protein is largely monomeric (Feng et al., unpublished results). Therefore, we conclude that in the concentration range employed in the present study, both apocytochrome b_{562} and ferricytochrome b_{562} exist in the monomeric state.

As the ferricytochrome b_{562} structure is highly asymmetric yet compact, changing to a more asymmetric structure would require partial unfolding of the tertiary structure. At the present time, it is difficult to distinguish the second and the third possibilities listed above, and they may well coexist in apocytochrome b_{562}. It is noted that a similar result has been reported for apocytochrome b_5 using the sedimentation method, where the protein also appears to undergo either an overall swelling or an increase in asymmetry upon removal of the heme (Huntley & Strittmatter, 1972).

Heat Capacity Change and Hydrophobic Core Size. The free energy of stabilization and the heat capacity change are coupled by the Helmholtz equation:

$$\Delta G^\circ = \Delta H(1 - T/T_m) - \Delta C_p[T_m - T + T \ln (T/T_m)] \quad (5)$$

Given the parameters determined from the thermal denaturation curves, the free energies of stabilization for apocytochrome b_{562} and ferricytochrome b_{562} at 20 °C are estimated to be 3.4 and 4.8 kcal/mol, respectively. While the value for the apoprotein is in good agreement with 3.2 kcal/mol extrapolated from the urea denaturation curve, that for the holoprotein is significantly lower than 6.6 kcal/mol derived in the urea unfolding experiment, perhaps due to the uncertainty in ΔC_p obtained using the van't Hoff approach at large ΔH [discussed by Pace and Laurents (1989)]. An estimate of ΔC_p can also be obtained from the Helmholtz equation, given T_m, ΔH_m, and ΔG° (Pace & Laurents, 1989). Using this method, a change in the specific heat capacity of 1.9–2.2 kcal/(mol·deg) was estimated for ferricytochrome b_{562}.

Privalov and his co-workers have demonstrated that the magnitude of the specific heat capacity change of a protein upon unfolding correlates with the size of the nonpolar hydrophobic core in the native protein (Privalov & Makhatadze, 1990). The smaller heat capacity change found for the apoprotein therefore indicates a decrease in the size of the hydrophobic core in the absence of the heme. An inspection of the holoprotein crystal structure suggests that the removal of the heme, without further structural change, exposes several buried hydrophobic residues to the solvent. A question arises whether such an exposure is responsible for the decrease in the hydrophobic core. We show below that it alone cannot account for the amount of decrease observed.

Quantitatively, the hydration heat capacity change ($\Delta^U_N C^h_p$), which is shown to be the major contributor to the observed heat capacity change of protein unfolding (Privalov & Makhatadze, 1990), can be calculated using the equation:

$$\Delta^U_N C^h_p = \Delta^U_N ASA_i \Delta C_{p,i} \quad (6)$$

where $\Delta^U_N ASA_i$ is the change in solvent-accessible surface area (ASA) for groups of type i in the protein upon complete unfolding and $\Delta^U_N C_{p,i}$ is the hydration heat capacity of the corresponding group per ASA unit calibrated by Makhatadze and Privalov (1990). Given the high-resolution crystal structure of ferricytochrome b_{562}, the expected heat capacity change of cytochrome b_{562} due to the hydration effect is estimated to be 1.9 kcal/(mol·deg) (heme contribution is assumed to be small and so is not included). Assuming the native cytochrome b_{562} structure is completely retained in the absence of the heme group, the calculation yields a heat capacity change of 1.8 kcal/(mol·deg). The change of 0.1 kcal/(mol·deg) is much smaller than the experimentally derived difference of at least 0.5 kcal/(mol·deg). More hydrophobic core than the heme crevice must be exposed to solvent in the absence of the heme. Considering the large amount of remaining secondary structure and the compactness of apocytochrome b_{562} structure, a more plausible proposal is that the removal of the heme results in a global "swelling" of structure, or a partially unfolded structure. Such a structure resembles the "molten globule" or the "collapsed form" described by Ptitsyn (1987), Kim and Baldwin (1990), and others.

In summary, since the secondary structure is largely intact in the apoprotein as confirmed by NMR studies (Feng et al., 1991), the major effect of heme binding appears to be on the tertiary structure, i.e., the packing of the helices. This can either be a dynamic expansion of the cytochrome b_{562} structure or be a rearrangement of the tertiary structure involving a partial exposure of the hydrophobic core in cytochrome b_{562}. Although the magnitude of the change in either secondary structure or molecular dimension is small, the effect of heme binding on the stability of cytochrome b_{562} is rather significant. Further description of apocytochrome b_{562} awaits the completion of the solution structure derived from NMR methods.

Acknowledgments

We thank Dr. Mark T. Fisher for providing his unpublished data and for many helpful discussions.

Registry No. Cytochrome b_{562}, 9064-79-3; heme b, 14875-96-8.

References

Ames, G. F.-L., Prody, C., & Kustu, S. (1984) *J. Bacteriol. 160*, 1181–1183.

Bullock, P. A., & Myer, Y. P. (1978) *Biochemistry 17*, 3084–3091.

Cocco, M. J., & Lecomte, J. T. J. (1990) *Biochemistry 29*, 11067-11072.
Demchenko, A. P. (1986) *Ultraviolet Spectroscopy of Proteins*, p 123, Springer-Verlag, Berlin.
Dyson, H. J., & Beattie, J. K. (1982) *J. Biol. Chem. 257*, 2267-2273.
Edelhoch, H. (1967) *Biochemistry 6*, 1948-1954.
Feng, Y., & Englander, S. W. (1990) *Biochemistry 29*, 3505-3509.
Feng, Y., Wand, A. J., & Sligar, S. G. (1991) *Biochemistry 30*, 7711-7717.
Fisher, M. T. (1991) *Biochemistry* (submitted for publication).
Goto, Y., Calciano, L. J., & Fink, A. L. (1990) *Proc. Natl. Acad. Sci. U.S.A. 87*, 573-577.
Griko, Y. V., Privalov, P. L., Venyaminov, S. Y., & Kutyshenko, V. P. (1988) *J. Mol. Biol. 202*, 127-138.
Harrison, S. C., & Blout, E. R. (1965) *J. Biol. Chem. 240*, 299-303.
Huntley, T. E., & Strittmatter, P. (1972) *J. Biol. Chem. 247*, 4641-4647.
Itagaki, E., & Hager, L. P. (1966) *J. Biol. Chem. 241*, 3687-3695.
Kim, P. S., & Baldwin, R. L. (1990) *Annu. Rev. Biochem. 59*, 631-660.
Lederer, F., Glatigny, A., Bethge, P. H., Bellamy, H. D., & Mathews, F. S. (1981) *J. Mol. Biol. 148*, 427-448.
Leutzinger, Y., & Beychok, S. (1981) *Proc. Natl. Acad. Sci. U.S.A. 78*, 780-784.
Makhatadze, G. I., & Privalov, P. L. (1990) *J. Mol. Biol. 213*, 375-384.
Mathews, F. S., Bethge, P. H., & Czerwinski, E. W. (1979) *J. Biol. Chem. 254*, 1699-1706.
Moore, C. D., & Lecomte, J. T. J. (1990) *Biochemistry 29*, 1984-1989.
Moore, C. D., Al-Misky, O., & Lecomte, J. T. L. (1991) *Biochemistry 30*, 8357-8365.
Myer, Y. P., & Bullock, P. A. (1978) *Biochemistry 17*, 3723-3729.
Nikkila, H., Gennis, R., & Sligar, S. G. (1991) *Eur. J. Biochem.* (in press).
Pace, C. N., & Laurents, D. V. (1989) *Biochemistry 28*, 2520-2525.
Privalov, P. L., & Makhatadze, G. I. (1990) *J. Mol. Biol. 213*, 385-391.
Provencher, S. W., & Glockner, J. (1981) *Biochemistry 20*, 33-37.
Ptitsyn, O. B. (1987) *J. Protein Chem. 6*, 273-293.
Schellman, J. A. (1987) *Biopolymer 26*, 549-559.
Teale, F. W. J. (1959) *Biochim. Biophys. Acta 35*, 543.
Yip, Y. K., Waks, M., & Beychok, S. (1972) *J. Biol. Chem. 247*, 7237-7244.

Hydrophobic Content and Lipid Interactions of Wild-Type and Mutant OmpA Signal Peptides Correlate with Their in Vivo Function†

David W. Hoyt‡,§ and Lila M. Gierasch*,‡,∥
Departments of Biochemistry and Pharmacology, University of Texas Southwestern Medical Center, Dallas, Texas 75235-9041
Received June 11, 1991; Revised Manuscript Received August 5, 1991

ABSTRACT: Peptides corresponding to the wild-type signal sequence of the *Escherichia coli* outer membrane protein OmpA and several mutants have been synthesized and characterized biophysically. The mutations were designed collaboratively with Inouye and co-workers to test the understanding of the critical characteristics of signal sequences required for their functions. The in vivo results for these mutants have been reported [Lehnhardt, S., Pollitt, S., & Inouye, M. (1987) *J. Biol. Chem. 262*, 1716-1719; Goldstein, J., Lehnhardt, S., & Inouye, M. (1990) *J. Bacteriol. 172*, 1225-1231; Goldstein, J., Lehnhardt, S., & Inouye, M. (1991) *J. Biol. Chem. 266*, 14413-14417], and the present paper compares the conformational and membrane-interactive properties of six of the OmpA signal peptides. Peptides corresponding to functional OmpA signal sequences in vivo are predominantly α-helical in membrane-mimetic environments and insert readily into phospholipid bilayers. Nonfunctional OmpA signal peptides may have high helical content but do not penetrate deeply into the acyl chain region of bilayers. The ability of the signal peptides to insert into membranes and their in vivo function correlate with the residue-average hydrophobicity of their hydrophobic cores. The results obtained on OmpA signal peptides parallel closely our previous observations on peptides corresponding to the LamB signal sequence and mutants, arguing that the critical biophysical properties of signal sequences are general despite their lack of primary sequence identity.

Despite considerable effort directed at elucidating the roles of signal sequences in protein export [for reviews see Gierasch (1989), Randall et al. (1987), Benson et al. (1985), Gennity et al. (1990), and Jones et al. (1990)], many questions remain. One of the major puzzles is how signal sequences, which lack primary sequence identity, can share several mechanistic steps in export. Recent genetic (Bieker & Silhavy, 1990) and biochemical (Hartl et al., 1990) evidence suggests that a multistage pathway is followed by a nascent exported protein: First, cytoplasmic chaperones such as SecB may bind the chain and help to keep it in a translocation-competent conformation (Collier et al., 1988; Kumamoto & Gannon, 1988). The signal sequence may be involved in this binding, but its presence is

† Supported by NIH Grant GM 34962 and by the Robert A. Welch Foundation.
* Corresponding author.
‡ Department of Biochemistry.
§ Present address: Department of Biochemistry, University of Alberta, Alberta T6E 2E3, Canada.
∥ Department of Pharmacology.

0006-2960/91/0430-10155$02.50/0